

## Precision measurement of the 1S Lamb shift and of the 1S-2S isotope shift of hydrogen and deuterium

C. Wieman\* and T. W. Hänsch

*Department of Physics, Stanford University, Stanford, California 94305*

(Received 14 September 1979)

A precision measurement of the 1S Lamb shift of atomic hydrogen and deuterium, using high-resolution laser spectroscopy is reported. The 1S-2S transition was observed by Doppler-free two-photon spectroscopy, using a single-frequency cw dye laser near 4860 Å with a nitrogen-pumped pulsed dye amplifier and a lithium formate frequency doubler. The  $n = 2-4$  Balmer- $\beta$  line was simultaneously recorded with the fundamental cw dye-laser output in a low-pressure glow discharge, using sensitive laser polarization spectroscopy. From a comparison of the two energy intervals a ground-state Lamb shift of  $8151 \pm 30$  MHz has been determined for hydrogen and  $8177 \pm 30$  MHz for deuterium, in agreement with theory. The same experiments yield a tenfold improved value of the 1S-2S isotope shift  $670992.3 \pm 6.3$  MHz and provide the first experimental confirmation of the relativistic nuclear recoil contribution to hydrogenic energy levels.

### I. INTRODUCTION

The measurement of Lamb shifts in hydrogenic atoms has played a vital role in the development of quantum electrodynamics (QED). Since the first measurement of the splitting between the  $2S_{1/2}$  and  $2P_{1/2}$  levels by Lamb and Retherford,<sup>1</sup> Lamb shifts have been measured for many hydrogenic states. Some of these measurements are among the most precise tests of quantum electrodynamics. One measurement which was notably missing, however, was that of the shift of the 1S ground state.

This paper reports on the last of a series of three increasingly precise measurements of this quantity performed at Stanford University. Unlike previous Lamb-shift measurements, these experiments are based on high-resolution laser spectroscopy. A first and rather preliminary experimental value of the 1S Lamb shift was obtained by Hänsch *et al.*,<sup>2</sup> at the time of the first observation of 1S-2S two-photon excitation in hydrogen. This was followed by the more careful measurement of Lee *et al.*,<sup>3</sup> combining the techniques of Doppler-free two-photon spectroscopy and saturated absorption spectroscopy.

In the present measurements we have made a number of important technical improvements which have enabled us to further reduce the uncertainty to  $\pm 30$  MHz. Among these improvements have been the development of a new, highly sensitive technique of Doppler-free laser spectroscopy, "polarization spectroscopy,"<sup>4</sup> and the construction of a cw dye-laser oscillator with pulsed dye-laser amplifier which offers substantially better power and bandwidth than the previously used pulsed dye-laser system. The new laser has also enabled us to measure the Lyman- $\alpha$  isotope shift for hydrogen and deuterium to within  $\pm 6.3$  MHz. This

result gives the first experimental confirmation of the relativistic nuclear recoil correction to hydrogenic energy levels.

Traditionally, Lamb shifts of S states have been measured by exciting radiofrequency transitions to a nearby P state. This technique cannot be used for the ground state, because there is no P state in the  $n = 1$  level, and a measurement of the 1S shift is consequently considerably more difficult. Herzberg<sup>5</sup> attempted the direct approach of measuring the absolute wavelength of the Lyman- $\alpha$  line to sufficient precision, but such an experiment is beset by many problems. First, the Lyman- $\alpha$  line (1215 Å) is in the vacuum-ultraviolet region of the spectrum where precision wavelength measurements are difficult. Secondly, traditional emission spectroscopy is complicated because emission sources are strongly self-reversed, while absorption spectroscopy is plagued by spurious background lines in continuum sources. Thirdly, the Doppler width of the Lyman- $\alpha$  line is about 40 GHz at room temperature, four times larger than the expected Lamb shift. And finally, if all these difficulties could be surmounted to obtain a precise value for the Lyman- $\alpha$  energy, the present uncertainty of the Rydberg constant<sup>6</sup> prevents one from determining the 1S Lamb shift to better than one part in 1000.

Recent advances in high-resolution laser spectroscopy together with improvements in dye-laser technology have made it possible to determine the 1S Lamb shift in a different manner, however, which avoids all these difficulties. This approach, as first described in Ref. 2, uses laser spectroscopy to precisely compare the Balmer- $\beta$  ( $n = 2$  to 4) transition energy with  $\frac{1}{4}$  of the Lyman- $\alpha$  energy. If the Bohr formula were correct these two intervals would be exactly the same,  $\frac{3}{16}$  of the

Rydberg energy. Actually they differ by the ground-state Lamb shift plus small, well-measured QED and fine-structure corrections to the excited-state energies. Thus an accurate comparison of the two intervals allows one to determine the 1S Lamb shift.

The comparison of the two energies is made using a powerful and highly monochromatic dye laser with a wavelength near 4860 Å as illustrated in Fig. 1. The frequency-doubled output of this laser is used to excite two-photon transitions from the 1S ground state to the metastable 2S state. Simultaneously, the fine-structure spectrum of the Balmer-β line is observed using the fundamental laser output, and the position of some component of this line is measured relative to the two-photon reso-

nance. As can be seen in Fig. 1, a major contribution to this separation originates from the 1S Lamb shift. Both wavelengths are near 4860 Å, and one avoids the problems of vacuum-ultraviolet spectroscopy. Furthermore, Doppler broadening of the 1S-2S transition can easily be avoided by excitation with counterpropagating beams.<sup>2</sup> And because the measurement only involves the comparison of two hydrogen transitions, the uncertainty of the Rydberg constant is unimportant.

## II. BACKGROUND

### A. Hydrogen energy levels and 1S lamb shift

The energy levels of hydrogen can be written in the form<sup>7</sup>

$$E(n, J, L) = E_D(n, J) + E_R(n) + E_N(n, L) + E_L(n, J, L), \quad (1)$$

where  $E_D$  is the energy predicted by the Dirac equation using the reduced mass Rydberg constant,  $E_R$  is the additional nuclear recoil correction predicted by the Breit equation for a relativistic two-body system,  $E_N$  is the correction due to nuclear size and nuclear structure effects, and  $E_L$ , a sum of many terms, gives the QED corrections. In this paper we will be somewhat loose with the term "ground-state Lamb shift," and use it to refer to the total deviation of the 1S energy from the Dirac energy, i.e., the sum  $E_R(1S) + E_N(1S) + E_L(1S)$ . A detailed list of all the known contributions to this shift with their most recently computed numerical values is given in Ref. 7. The relativistic nuclear recoil term is given to lowest order by

$$E_R = -\frac{m}{M} \frac{\alpha^4}{8n^4} mc^2, \quad (2)$$

where  $m$  is the electron mass and  $M$  the nuclear mass. This recoil shift, which has never been experimentally verified, amounts to  $-23.81$  MHz for hydrogen 1S and  $-11.92$  MHz for deuterium 1S. The respective 1S shifts due to nuclear structure are  $1.00 \pm 0.05$  and  $6.78 \pm 0.09$  MHz. Including these corrections, the 1S Lamb shift has a theoretical value of  $8149.43 \pm 0.08$  MHz for hydrogen and  $8172.23 \pm 0.2$  MHz for deuterium.

The previous measurements of the 1S Lamb shift and the nonlinear spectroscopic techniques involved in this work have been discussed elsewhere in various degrees of completeness.<sup>2, 3, 8, 9</sup> However, for the sake of clarity we shall give a brief review.

### B. Doppler-free two-photon spectroscopy of 1S-2S

The technique of Doppler-free two-photon spec-

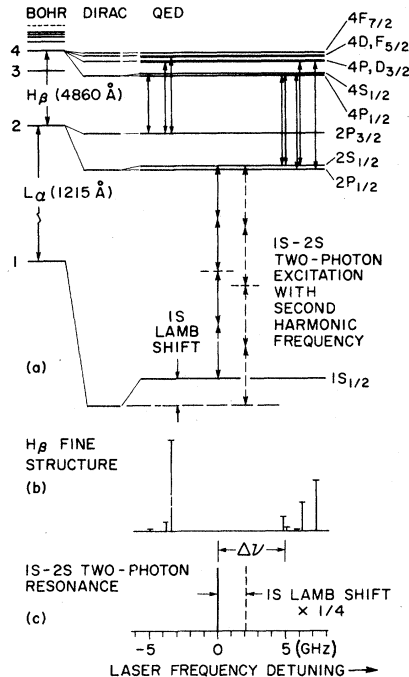


FIG. 1. Top: Simplified diagram of hydrogen energy levels and transitions. The Dirac fine structure and QED corrections for  $n=1, 2$ , and  $4$  are shown on an enlarged scale. Hyperfine structure and Stark effect are ignored, except for showing the weakly Stark-allowed transition  $2S_{1/2} - 4S_{1/2}$ . Bottom: Fine-structure spectrum of the Balmer-β line and relative position of the 1S-2S two-photon resonance as recorded with the second harmonic frequency. The dashed line and the dashed arrows above give the hypothetical position of the 1S-2S resonance if there were no 1S Lamb shift. An experimental value of the 1S Lamb shift has been determined from the frequency interval  $\Delta\nu$  between the two-photon resonance and a crossover resonance observed in a polarization spectrum of Balmer-β halfway between the fine-structure components  $2S_{1/2} - 4P_{1/2}$  and  $2S_{1/2} - 4S_{1/2}$ .

troscopy, reviewed in Ref. 10, has been central to all measurements of the 1S Lamb shift. First suggested by Vasilenko *et al.*,<sup>11</sup> two-photon excitation of gas atoms with two counterpropagating laser beams can provide narrow resonance signals free of first-order Doppler broadening, because the atoms see the two beams with opposite, and thus canceling, Doppler shifts.

Two-photon excitation of hydrogen 1S-2S requires ultraviolet radiation near 2430 Å of relatively high intensity, because there is no near-resonant intermediate level. The transition rate for cw excitation has been computed numerically by several authors.<sup>12,13</sup> According to Gontier and Trahin,<sup>12</sup> the two-photon absorption cross section is of the order

$$\sigma(A) \approx 2.75 \times 10^{-17} I g \text{ cm}^2, \quad (3)$$

where  $I$  is the light intensity in  $\text{W}/\text{cm}^2$  and  $g$  the inverse atomic transition linewidth in sec.

The expected natural linewidth of the 1S-2S transition in the absence of collisions is only about 1 Hz, limited by the  $\frac{1}{7}$ -sec lifetime of the 2S state. While currently available lasers are much too broadband to reach this limit, they are more than sufficient to observe the transition. For a pulsed laser we can easily estimate the excitation probability with the help of time-dependent second-order perturbation theory.<sup>14</sup> Assuming, for simplicity, a square excitation pulse of time duration  $T$ , intensity  $I$ , frequency  $\omega$ , and transform limited bandwidth  $\Delta\omega = \pi/T$  we obtain an excitation probability per atom

$$P = \sigma(A) \frac{I}{\hbar\omega} \frac{1}{2g} \frac{4 \sin^2[(2\omega - \omega_{1S-2S})\frac{1}{2}T]}{(2\omega - \omega_{1S-2S})^2}, \quad (4)$$

where  $\omega_{1S-2S}$  denotes the atomic resonance frequency. At exact resonance, the rightmost fraction simplifies to  $T^2$ ; i.e., the effective absorption cross section, compared to the steady-state result (Eq. 3), is reduced by a factor  $T/2g$ . With a pulse length of 7 nsec and an intensity  $I = 2 \times 10^6 \text{ W}/\text{cm}^2$  (approximately the experimental conditions), we find an excitation probability per atom of about  $2 \times 10^{-3}$ . Since the density of 1S atoms can easily be as large as  $10^{14}/\text{cm}^3$ , the signal can be substantial even if the detection efficiency is poor.

#### C. Previous measurements of the 1S Lamb shift and limitations

In both previous measurements of the 1S Lamb shift,<sup>2,3</sup> the frequency-doubled output of a pulsed dye-laser oscillator-amplifier system<sup>15</sup> was used to excite the 1S-2S transition, and the excitation was detected by observing the Lyman- $\alpha$  radiation emitted in the collision-induced 2S-1S decay.

In the first experiment,<sup>2</sup> the 1S-2S interval was compared with the  $n=2-4$  interval by simply recording a Doppler-broadened absorption of the Balmer- $\beta$  line in a glow discharge plasma, using the fundamental dye-laser output. The second measurement<sup>3</sup> achieved a substantial improvement in accuracy by using the technique of saturated absorption spectroscopy to obtain better resolution of the Balmer- $\beta$  line, again with a portion of the fundamental dye-laser beam. But despite sub-Doppler linewidths, the fine structure of this line remained partly unresolved, and the quoted accuracy of the 1S Lamb shift was still almost entirely limited by the inadequate resolution of this reference line.

#### D. Laser polarization spectroscopy

Searching for ways to improve the resolution of the Balmer- $\beta$  line, we developed the technique of laser polarization spectroscopy,<sup>4</sup> a method of Doppler-free spectroscopy which offers considerably higher sensitivity than conventional saturated absorption spectroscopy. This technique enabled us to observe the Balmer- $\beta$  line with a low-power cw dye laser in a mild glow discharge. Single Stark components of fine-structure lines could be readily resolved in the small axial electric field of the discharge plasma. This success opened the way for the present improved measurement of the 1S Lamb shift.

The basic concept of polarization spectroscopy is rather simple: A linearly polarized probe laser beam is sent through a gas sample and passes through a nearly crossed linear polarizer, before reaching a detector. Any optical anisotropy in the sample which changes the probe polarization can thus be detected with high sensitivity.

Such an anisotropy is introduced by a second laser beam of the same frequency, which is counterpropagating and circularly polarized. In this case, assuming low intensities, one detects a Doppler-free signal as given by Eq. (4) of Ref. 4:

$$I = I_0 \left[ \theta^2 + \theta \frac{s}{2} \frac{x}{1+x^2} + \left( \frac{s}{4} \right)^2 \frac{1}{1+x^2} \right], \quad (5)$$

where  $I$  is the detected intensity,  $I_0$  the incident probe intensity, and  $\theta$  is the rotation angle of the analyzing polarizer from the perfectly crossed orientation. The frequency detuning from the center of the Doppler-broadened line is described by the normalized parameter  $x = (\omega - \omega_{ab})/\gamma_{ab}$ , where  $\omega$  is the laser frequency,  $\omega_{ab}$  is the transition frequency, and  $\gamma_{ab}$  is the natural linewidth of the transition. The parameter  $s$  gives the maximum relative intensity difference between the right- and left-circularly-polarized components of the probe and is defined by  $s = -\frac{1}{2}(1-d)\alpha_0 l I/I_{\text{sat}}$ , where  $l$  is the sample length,  $\alpha_0$  is the unsaturated

absorption coefficient at line center,  $I_{sat}$  is the transition saturation parameter, as defined in Ref. 15, and  $d$  is the ratio of the light-induced changes in the absorption coefficient for right- and left-circularly-polarized light.

In the chosen mode of operation the analyzing polarizer is rotated so that  $\frac{1}{2}\theta s$  is about 10 times larger than  $(s/4)^2$ , and a derivative signal is obtained by giving the laser a small frequency modulation and recording the corresponding signal modulation with a phase sensitive amplifier. The resulting line shape, the derivative of  $x/(1+x)$ , appears bell shaped with inverted wings, and its width is less than  $\frac{1}{2}$  the natural linewidth.

### III. APPARATUS

A schematic overview of the apparatus is given by Fig. 2. The output of a single-frequency cw dye laser (upper left) is split into four beams. One of these is sent into a frequency-marker interferometer (top) for the purpose of calibration. Two of the beams become the polarizing and probe beam of the polarization spectrometer (center). Finally, the fourth beam provides the input for a pulsed dye-laser amplifier system. The amplified beam is sent through a frequency-doubling crystal which generates the ultraviolet radiation for the two-photon spectrometer (bottom right). Because of its complexity, this entire setup is spread over three separate optical tables.

#### A. cw dye-laser oscillator

The cw laser is a Spectra Physics model 375 folded cavity jet stream dye laser which has been modified to provide tunable single-frequency operation at blue wavelengths, using a solution of 7-diethylamino-4-methylcoumarin in ethylene glycol. The standard tuning elements, a dielectric tuning wedge filter and a 0.1-mm uncoated quartz etalon are augmented by two additional intracavity etalons. The first is an angle-tuned solid uncoated quartz etalon 0.5 mm thick. The second is an air spaced etalon with a gap of 5 mm (free spectral range 30 GHz) and 30% mirror reflectivity. The spacing can be varied with a piezotransducer, and the etalon is contained in a temperature stabilized oven. For cavity fine tuning the laser output mirror is mounted on a piezotransducer. To decrease the linewidth the entire laser is completely enclosed in a large, nearly airtight, wooden box.

The dye laser is pumped by a Spectra Physics model 171 argon-ion laser. The pump threshold for single-frequency operation at 4860 Å is about 600 mW. An output of 20 mW is obtained with 2-W pump power. During the experiment the dye laser

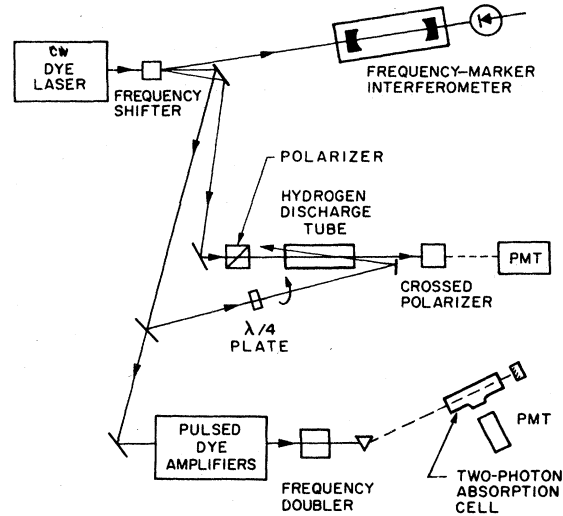


FIG. 2. Schematic of experiment. The Balmer- $\beta$  line is recorded by polarization spectroscopy (center), while the 1S-2S transition is observed by two-photon excitation with the second harmonic of the dye-laser frequency (bottom).

operated typically at 7.5-mW output power.

The dye-laser frequency can be continuously scanned over 4 GHz by applying tuning ramp voltages to the piezotransducers of the cavity end mirror and the air spaced etalon. During the experiment the linewidth was on the order of 5 to 10 MHz [full width at half maximum (FWHM)], although the width decreased to about 2 MHz when the pneumatic vibration isolation of the optical table was activated. The frequency modulation (about 10-MHz sweep amplitude) needed to record a derivative signal is obtained by adding an audio frequency ac voltage (4 V, 2 kHz) to the ramp voltage of the cavity mirror.

The dye-laser output beam is sent into an acousto-optic modulator. Diffraction from a traveling acoustic wave in a crystal of fused quartz generates three beams, one upshifted in frequency (+37.60 MHz), one downshifted (-37.60 MHz), and one with its frequency unchanged. The primary function of this device in our experiment is that of a beam splitter, but the frequency shift improves the signal-to-noise ratio of the polarization spectrometer, as will be discussed later. The upshifted beam, containing about 0.75 mW of power, is sent into the frequency-marker interferometer. The downshifted beam (also 0.75 mW) becomes the probe beam of the polarization spectrometer, while the unshifted beam is used as the polarizing beam. About 30% of this unshifted beam is split off with a partly reflecting mirror and sent into the pulsed amplifier system.

### B. Frequency-marker interferometer

The frequency-marker interferometer is a semi-confocal interferometer, consisting of two dielectric mirrors cemented onto the ends of a quartz tube. It has a finesse of 15, and its transmission peaks are separated by 113.142 33(15) MHz. This separation was used for frequency calibration in all reported measurements. The thermal drift of this frequency marker was 0.2 to 1.5 MHz/min and typically remained constant to better than 10% over 5 h.

The marker separation was determined to within 2 parts in  $10^4$ , by mechanically measuring the length of the spacer. To find a more accurate value, the dye laser was tuned to the center of a transmission peak, and the laser frequency was measured with a precise fringe-counting digital wave meter.<sup>16</sup> Then the laser was tuned to another peak, about  $10^3$  fringes away, and the frequency was measured again. From the frequency difference and the known marker spacing the number of fringes between the two peaks can be determined exactly, which in turn yields an improved marker separation. The procedure can then be repeated with a new, larger frequency interval. Taking several iterative steps in this manner, the separation between adjacent orders could be quickly determined to the quoted accuracy.

### C. Hydrogen discharge tube

In order to observe the Balmer- $\beta$  line in absorption, hydrogen atoms are excited in a Wood-type glow discharge tube, similar to those described in Refs. 6 and 9. The tube is 138-cm long with an inner diameter of 1.5 cm, and the walls are coated with orthophosphoric acid to prevent catalytic recombination of the atoms. Wet molecular hydrogen from an electrolytic generator provides a continuous gas flow through the tube. A large area cold aluminum cathode ensures a stable discharge.

The laser beams pass through a 60-cm-long center section of the positive discharge column. The windows are formed by pieces of quartz microscope slides, cemented onto tube extensions with Torr Seal adhesive. By gently squeezing these windows with small transverse clamps their birefringence can be reduced until extinction ratios better than  $10^{-7}$  are observed between crossed polarizers.

During the experiment the tube was operated at pressures between 0.1 and 1.0 torr and at currents between 5 and 20 mA, and the absorption at resonance ranged from as high as 10% to less than 1%, depending on pressure and current.

### D. Polarization spectrometer

A simplified scheme of the polarization spectrometer is included in Fig. 2. The polarizing beam is sent through a quarter wave plate to change its polarization from linear to circular. Two lenses of focal length  $f=7.8$  cm form a 1:1 telescope (not shown in Fig. 2) which focuses the beam (original diameter 3 mm) to a waist diameter of about 0.2 mm at the center of the hydrogen discharge tube at 75-cm distance. The probe beam, coming from the opposite direction, passes through an identical telescope to nearly match the confocal parameters of the polarizing beam. To ensure nearly perfect linear polarization the probe is sent through a prism polarizer before entering the discharge tube. It crosses the polarizing beam near the center of the discharge tube at an angle of 2 mrad. After emerging from the Wood tube, the probe is sent into a second, "analyzing" polarizer whose axis is rotated nearly 90 degrees relative to the first one.

Both polarizers are cemented Glan Thomson prism polarizers (Karl Lambrecht) with a rated extinction ratio of  $10^{-5}$ . By using small (about 2-mm diameter) and fairly well collimated beams, however, we typically achieve extinction ratios better than  $10^{-7}$ . During the experiment, the angle of the analyzing polarizer was adjusted so that the  $\theta_s$  contribution to the signal<sup>6</sup> was about 5 to 10 times larger than the  $s^2$  contribution. This angle depended on the experimental conditions and varied between  $4 \times 10^{-4}$  and  $3 \times 10^{-3}$  rad.

Probe light which passes through the analyzing polarizer is sent through a spatial filter at 1.5-m distance from the discharge tube (lens of  $f=7.8$  cm, pinhole of 50- $\mu$ m diameter), and its intensity is monitored by a photomultiplier (RCA 1P28) followed by a lock-in amplifier (PAR model JB5). The internal sine wave reference of this amplifier provides the signal for the 2-kHz dye-laser frequency modulation.

Although this apparatus can be assembled quite easily, certain pains must be taken to attain the large signal-to-noise ratio offered by polarization spectroscopy. The first requirement is a good extinction ratio for the probe beam. Considering the small rotation angle of the analyzing polarizer it is obvious that an extinction ratio much worse than  $10^{-7}$  would have been a serious limitation in the reported experiments. Several different measures are taken to assure this ratio: First, fairly good polarizers are used and the beams through them are kept small and collimated; second, there are as few optical components as possible in between the polarizers, and for those which are unavoidable (the discharge windows) the birefringence

is minimized; finally, all surfaces are kept clean to avoid depolarizing scattering.

It is also important to minimize any light other than the probe light which reaches the detector. The two primary sources of such background in the present experiment are the gas discharge and backscattering of the polarizing beam. The spatial filter reduces the light from both these sources to below the residual probe intensity ( $10^{-7} I_0$ ). Originally we were facing the problem, however, that the small amount of scattered polarizing light which still reached the detector was coherent with the probe light, causing the detector to respond to an interference between the two electric fields. Slow phase fluctuations resulted in considerably increased noise. The use of the acousto-optic frequency shifter eliminates this problem by causing the interference term to oscillate at a frequency too high for the detector to respond to it. We found that vibrating one of the mirrors reflecting the polarizing beam, for instance, by mounting it on a radio speaker, also eliminates this noise source. The frequency shifter is preferred, however, because it also reduces amplitude fluctuations of the dye laser due to feedback into the cavity, a problem to which this dye laser is particularly sensitive.

#### E. Pulsed dye-laser amplifier

The pulsed laser amplifier is shown in Fig. 3. The system worked at first try more than adequately for this experiment, and little effort was made to optimize the geometry. The pump source is a Moletron UV 1000 nitrogen laser operating at 15 pulses per sec and producing 10-nsec-long pulses of about 650-kW peak power. Approximately 10% of this light is used to pump the first dye amplifier stage, 30% is sent to the second, and 60% to the third stage. The dye cells and the transverse focusing of the pump light into them are identical to those used in the pulsed oscillator-amplifier forerunner of this system.<sup>17</sup>

With 1-mW cw input power a gain of about  $10^5$  in peak power is readily achieved in the first stage, but the pulse width is only about 3–4 nsec (FWHM). The power of the amplified beam after the first stage is about 5 to 10 times larger than the amplified spontaneous fluorescence into the same solid angle. The second stage gives a (saturated) gain of about 45 and some pulse stretching, while the third stage gives a gain of 22 and stretches the pulse to about 7 nsec (FWHM). The third stage is saturated to such an extent that it produces the same peak power under almost any alignment condition. Optimizing the alignment broadens the roughly Gaussian-shaped pulse in time, however, and reduces the bandwidth accordingly, as we

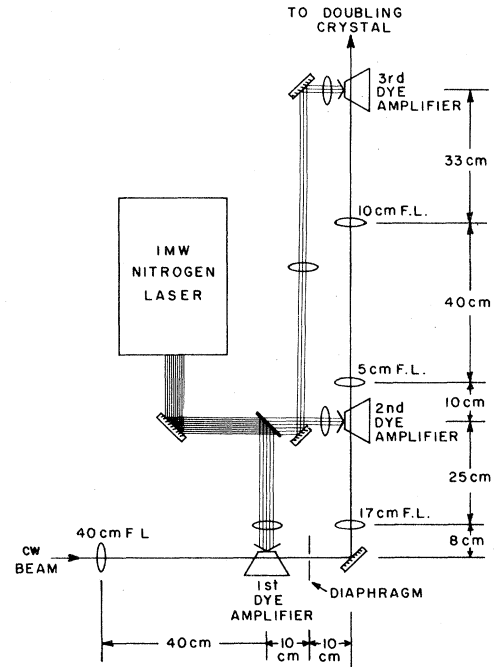


FIG. 3. Pulsed dye-laser amplifier.

found empirically. Pulse energies of about 5 mJ with less than 5% fluctuations are easily obtained, and the spatial beam profile can show a much closer resemblance to a Gaussian TEM<sub>00</sub> mode than was normally attained with the earlier pulsed oscillator-amplifier system.

In hindsight the most serious problem in the present experiment is the fact that the pulsed amplifiers not only broaden but also shift and distort the spectrum. To monitor this shift, a portion of the amplified output beam is sent through a confocal interferometer (2-GHz free spectral range, finesse 150) as indicated in Fig. 4. The transmitted light is measured by two photodiodes; one of these records the pulsed light while the other registers only the simultaneously present collinear cw light. Thus, as the laser is scanned over the transmission peak of the interferometer, the pulsed and cw spectra are obtained simultaneously and can be compared.

#### F. Two-photon spectrometer

Also shown in Fig. 4 are details of the two-photon spectrometer which is almost identical to that used in the earlier experiments.<sup>2,3</sup> The output of the pulsed amplifier is focused into a lithium formate frequency-doubling crystal (Lasermetrics) using a lens of  $f=18$  cm. The crystal is 1 cm long and phase matching near 4860 Å is achieved through angle tuning. With this geometry

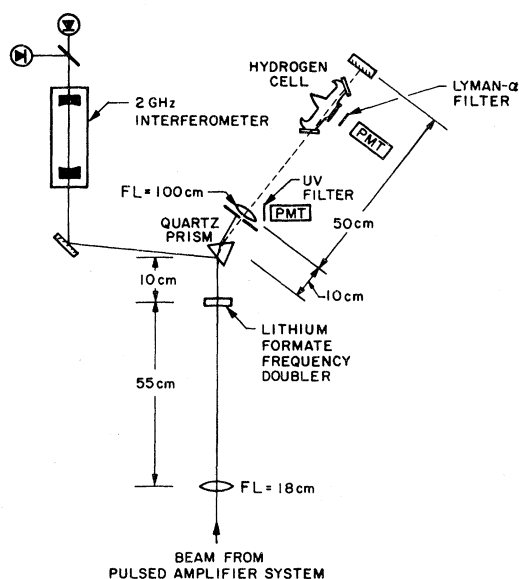


FIG. 4. Details of two-photon spectrometer.

the doubling efficiency approached 2%, and most data were taken at pulse energies of about  $7 \mu\text{J}$ . The crystal showed signs of burning after about 15 000 pulses at such a power level. (With tighter focusing it was possible to obtain over 7% conversion efficiency, but the crystal burned much more rapidly.)

The generated ultraviolet beam is separated from the fundamental beam by a Brewster-angle quartz prism and then collimated with a Suprasil lens ( $f=1000 \text{ mm}$ ). The ultraviolet intensity is monitored by observing the light reflected off this lens with a photomultiplier with attenuating diffuser. As it passes through the hydrogen absorption cell the beam has a nearly rectangular cross section of 0.2 by 0.4 mm. A flat mirror immediately after the cell is used to reflect the beam back onto itself to provide the required standing-wave field.

The two-photon absorption cell is the same as described in Refs. 2 and 3. The ground-state hydrogen atoms are produced in a Wood-type discharge and flow and diffuse into the absorption cell through a 25-cm-long folded transfer tube, coated with phosphoric acid. The discharge was run with a current of 20 mA and at pressures between 1.0 and 0.05 torr of wet hydrogen. The absorption cell is about 10 cm long with quartz windows for the ultraviolet beams on the ends set at the Brewster angle. The  $1S-2S$  excitation is monitored by observing the Lyman- $\alpha$  radiation emitted through a magnesium fluoride side window.

The vacuum-ultraviolet radiation is due to collisional mixing of the  $2S$  and  $2P$  states. From measurements of the collision cross sections<sup>18</sup> we

expect a  $2S$  lifetime of about 10 nsec at a pressure of 0.1 torr, which seems to agree with our (imprecise) observations. However, there is substantial radiation trapping and loss of photons through nonradiative decay mechanisms which are not well understood. To minimize this loss of signal the ultraviolet beams are kept as close to the side window as possible (distance less than 1 mm).

The emerging Lyman- $\alpha$  photons are detected with a solar blind photomultiplier (EMR 541J). Scattered laser light is reduced to a negligible level by a Lyman- $\alpha$  interference filter in front of the detector (Matra Seavom Co., 15% peak transmission,  $90 \text{ \AA}$  bandwidth). The output current from the photomultiplier is sent into a gated integrator.

#### G. Data processing

All data from the experiment, are converted into digital form (12 bits accuracy) and stored on magnetic disk for processing with a minicomputer (Hewlett-Packard 2100A).

#### IV. EXPERIMENTAL PROCEDURE AND ANALYSIS

A major portion of our efforts were devoted to the investigation of systematic line shifts, as summarized in Table I. The experimental procedure was divided into five distinct portions; the investigation of systematic shifts of the hydrogen two-photon line, the measurement of the separation of hydrogen and deuterium two-photon lines, the study of shifts of the Balmer- $\beta$  reference line, the measurement of the separation between the hydrogen two-photon line and the Balmer- $\beta$  reference line, and finally, the measurement of the hydrogen-deuterium separation of the Balmer- $\beta$  line. The result of the first two parts gives the H-D  $1S-2S$  isotope shift while the first, third, and fourth part yield the hydrogen  $1S$  Lamb shift. The deuterium  $1S$  Lamb shift is obtained by combining results of all five portions.

##### A. Systematic shifts of the $1S-2S$ line

The only systematic shift of the two-photon signal studied experimentally was that due to the pressure in the two-photon absorption cell. First the pressure was set at 0.05 torr and the laser was scanned  $\sim 5$  times over an  $\sim 1$ -GHz range containing the resonance line. During these scans the computer sampled the inputs to six channels on the analog to digital converter 100 times per sec. Each sweep lasted  $\sim 25$  sec so the sampling points were about 0.25 MHz apart. The six data inputs were the two-photon signals, the intensity of frequency-doubled ( $2430\text{-\AA}$ ) light, the frequency-marker signal, the pulsed signal from the spectrum analyzer monitoring the amplified beam, the cw signal from

TABLE I. Systematic line shifts considered.<sup>a</sup>

1S-2S two-photon resonance			
pressure	meas	0 ± 5	MHz/torr
ac Stark effect	calc	+0.6	MHz/MW cm <sup>-2</sup>
laser line shape	meas/calc	-13 ± 9%	of linewidth
Balmer-β line (4S <sub>1/2</sub> -2S <sub>1/2</sub> -4P <sub>1/2</sub> crossover)			
polarizer angle	meas <sup>b</sup>	15 ± 4	MHz/sθ <sup>-1</sup>
polarizer angle	calc <sup>b</sup>	12	MHz/sθ <sup>-1</sup>
pressure, electric field	meas <sup>c</sup>	-28 ± 6	MHz/torr
zero-pressure Stark shift and unresolved hyperfine structure	calc <sup>c</sup>	-4.5 ± 2	MHz
ac Stark effect	calc	-0.28	MHz/W cm <sup>-2</sup>
discharge current	meas <sup>c</sup>	-0.1 ± 0.2	MHz/mA
frequency-marker thermal drift	meas <sup>d</sup>	60 ± 1	MHz/h

<sup>a</sup>Shift  $\nu$  (observed) -  $\nu$  (true) in terms of fundamental dye-laser frequency.

<sup>b</sup>Good approximation for  $|s\theta^{-1}| < 0.2$ , as in all measurements. See Eq. (5).

<sup>c</sup>These results are not independent. See text for discussion.

<sup>d</sup>Typical value for a given run.

that analyzer, and last, the scanning voltage applied to the cw laser end mirror piezodrive. All pulsed signals were processed by gated integrators. The output proportional to the pulse area was held constant in between laser pulses. After recording these scans the pressure was changed to 1.0 torr and 5 more scans were made with the same recording procedure. This was followed by 5 scans again at 0.05 torr and then 5 at 1.0 torr. The entire procedure took about 30 min.

The first step in the analysis of these data was to set the frequency scale for each scan by finding the centers of the frequency-marker peaks. For each peak the computer generated a smoothed curve where each point of the smoothed curve was the average of 10 adjacent raw data points. For example, the 95th point on the smoothed curve was the average of the 91st through 100th raw data points. The line center for the smoothed curve was found at the  $\frac{1}{4}$ ,  $\frac{1}{2}$ , and  $\frac{3}{4}$  peak-height points and the average of these points was taken to be the frequency-marker center. Although there was essentially no uncertainty in finding the center of a given peak, imperfections in the laser piezodrive caused a 2-3% random fluctuation in the peak-to-peak spacing causing a corresponding uncertainty of the frequency scale. All subsequent analysis in this and the remaining part of the experiment was done in terms of frequency scales determined using this procedure.

The two-photon spectra were first normalized by dividing the signal by the square of the 2430-Å intensity. This caused no observable shift of the lines, but did reduce the pulse to pulse amplitude fluctuations slightly. Next the spectra were

smoothed in the same manner as used with the frequency marker except that a 40-point average was used. While such a smoothing routine could conceivably cause the peak frequency to shift, for our lineshapes the shift would be less than 0.4 MHz and hence negligible compared to the statistical uncertainty. Examples of such spectra are shown in Figs. 5 and 6(b). After smoothing, the centroid of the line including both hyperfine components was calculated. The values for each set of 5 runs were averaged and the resulting four points (at 0.05, 1, 0.05, and 1 torr) were plotted as a function of the time of acquisition to determine the thermal drift of the frequency marker. The drift rates shown by the high- and low-pressure points were the same, and an appropriate correction was made.

#### B. Hydrogen-deuterium 1S-2S isotope shift

The next stage of the experiment was the measurement of the 1S-2S isotope shift. For this, the

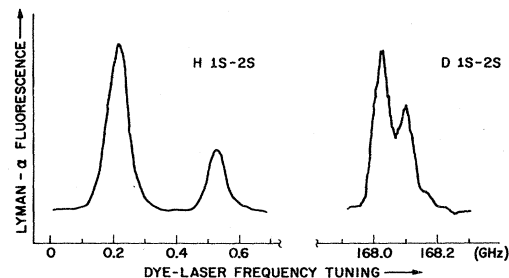


FIG. 5. Two-photon spectrum of 1S-2S transition in hydrogen (left) and deuterium (right).



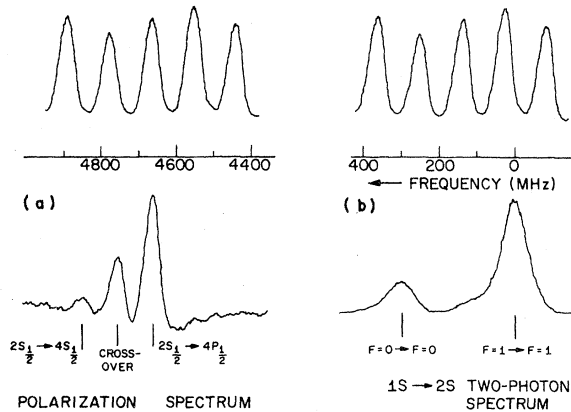


FIG. 6. (a) Portion of the polarization spectrum of the hydrogen Balmer- $\beta$  line. (b) Two-photon spectrum of hydrogen 1S-2S transition. The frequency-marker signal at the top has been recorded simultaneously.

two-photon absorption cell was filled with a mixture of H and D at 0.05 torr. A crude preliminary measurement using a digital wave meter was made to determine the separation of the hydrogen and deuterium lines to within one free spectral range of the frequency marker. The following procedure was then used to determine the additional fraction. Several (4 to 5) scans of the hydrogen two-photon line were made and the spectra stored as previously described and then the laser frequency was shifted to the deuterium line and the procedure repeated. The laser wavelength was returned to the hydrogen line and the sequence repeated until a total of 52 spectra were obtained.

The data were analyzed by finding the frequency scale and normalizing and smoothing the two-photon spectra just as before. At this stage in the analysis however, it was necessary to confirm that the deuterium and hydrogen line shapes were not systematically different (except for the difference in hyperfine splitting, of course). Because the two-photon line shape was not simple and could change noticeably over periods on the order of a day such a confirmation that it did not change with wavelength was necessary. This was verified by two tests. First, spectra of the fundamental pulsed laser taken at the wavelength of the hydrogen line, the deuterium line, and  $\sim 100 \text{ \AA}$  on either side were compared and found to be identical. While it is impossible to make a direct correspondence between this spectrum and the two-photon line shape, as will be discussed later, it was observed that changes in one were always correlated with changes in the other. The second test was to compare the two two-photon line shapes directly, a procedure which was complicated by the deuterium hyperfine splitting being

only partially resolved. This problem was surmounted by taking the line shape observed for a single hydrogen hyperfine component and using it to generate a predicted deuterium spectrum using the known hyperfine splitting and intensity ratio for deuterium. The generated line shape was then compared with the observed deuterium spectra obtained at similar times using only the overall amplitude as a free parameter. These were found to match to within the statistical fluctuations, confirming that the hydrogen and deuterium line shapes were the same. Now the centroids of the lines were calculated and these values plotted as a function of time. The drift of the frequency marker was then calculated and appropriate corrections made.

### C. Systematic shifts of Balmer- $\beta$ line

The next and longest portion of the experiment was the investigation of systematic shifts of the Balmer- $\beta$  signals. The basic procedure was to repeatedly scan the cw dye laser to obtain a polarization spectrum containing the  $2S_{1/2} \rightarrow 4P_{1/2}$  line, the  $2S_{1/2} \rightarrow 4S_{1/2}$  line (Stark allowed), and their crossover,<sup>19</sup> while changing various parameters [see Fig 6(a)]. We restricted ourselves to these lines because they are narrow and much simpler to interpret than the other components. During each scan the computer sampled and stored the inputs to three channels on the analog-to-digital converter (ADC) at 100 times/sec. The three inputs were the laser scanning voltage, the frequency-marker signal, and the output of the lock-in amplifier monitoring the polarization spectrometer phototube.

The first systematic effect studied was the shift of the polarization spectra line centers due to the addition of the small derivative-shaped  $S\theta$  term to the larger bell-shaped  $S^2$  term. To measure this shift several scans were made with the polarizer in the  $+\theta$  orientation then it was rotated to  $-\theta$ , which causes a shift in the opposite direction, and several more scans were recorded. This was repeated at several times to determine the frequency-marker drift, and at a variety of angles.

The following analysis procedure of the polarization spectra was used for this and all subsequent portions of the experiment. First the spectra were smoothed in the standard way. Between one and ten points were used in the smoothing average, depending on experimental conditions, with tests made to ensure this introduced no line shifts. The line center was then determined at regular height intervals (every 5% of the  $2S_{1/2} \rightarrow 4P_{1/2}$  line and every 10% of the crossover) and the average of these centers found.

The result of the tests of the  $\theta$  dependence

showed that for all values of  $\theta$  used in the subsequent measurements the shift was less than 3 MHz, in agreement with the theoretical estimates. As part of all subsequent measurements the data were taken with the polarizer in both + and - orientations and the results averaged, thereby canceling the shift to within a negligible uncertainty.

The effects of the discharge environment (current, pressure, electric field) on the Balmer- $\beta$  reference line were also investigated. First the effect of the current was studied by recording a series of spectra at discharge currents of 20 and 11 mA, alternating repeatedly between the two settings.

Next the effects of the pressure and the electric field in the discharge were measured. Because only the pressure could be independently varied and this in turn affected the electric field it was necessary to obtain a composite correction. In these measurements the same data-acquisition procedure was used as for the current shift measurements, except that the current was set at 11 mA and the pressure varied. Two data runs were used; one which took data at 0.16, 0.41, and 0.70 torr and the second at 0.39, 0.27, and 0.72 torr. The pressure readings were made using a thermocouple gauge. A total of 80 spectra were recorded.

#### D. Comparison of 1S-2S transition with Balmer- $\beta$ line

The fourth stage of the experiment was the measurement of the separation between the hydrogen two-photon peak and the crossover line between the  $2S_{1/2} \rightarrow 4P_{1/2}$  and the  $2S_{1/2} \rightarrow 4S_{1/2}$  transitions. This crossover was chosen as the reference line for the Lamb-shift measurement because it was less sensitive to the electric field perturbation than the other lines. In this stage seven data channels were read into the computer; the combination of the three cw and four pulsed data lines previously described. The two-photon absorption cell was operated at 0.05 torr and the polarization spectrometer discharge ran at 0.27 torr and 11 mA. 1-GHz scans with the same sampling rate as before were used. First, 5 scans were made over the two-photon line; then as rapidly as possible ( $\sim 1$  min) the laser wavelength was reset and the Balmer- $\beta$  crossover line was scanned several times. Examples of such spectra are shown in Fig. 6. The laser was then reset to the two-photon line and the procedure repeated until a total of 45 two-photon spectra and 51 Balmer- $\beta$  spectra were obtained.

The Balmer- $\beta$  spectra were analyzed using the same procedure as before, but it was necessary to use a different procedure in the analysis of the two-photon lines because of their asymmetric line shape. The difficulties caused by this line shape

will be discussed in Sec. V. After normalizing and smoothing the two-photon spectra as before, the line centers were found at equal intervals in the region between 30 and 90% of the peak height. This region was used because at lower than 30% the peak is dramatically skewed towards lower frequency, while above 90% the amplitude fluctuations make a center meaningless. The 10 center points could usually be fit with a straight line to within statistical fluctuations. This line was extrapolated to the peak maximum and that point taken to be the "peak" frequency. This value was typically about 5 MHz higher in frequency than the line center at the 50% point. Once these centers were found the data were averaged and graphed as before. Since this data run lasted several hours the frequency-marker drift was fit with a second-order polynomial (the second-order correction was about the same size as the statistical spread), and the data corrected.

#### E. Hydrogen-deuterium Balmer- $\beta$ isotope shift

The last quantity measured was the isotope shift between the hydrogen and deuterium Balmer- $\beta$  lines. For this the polarization spectrometer discharge was operated with a 50-50 mixture of hydrogen and deuterium. Polarization spectra of the  $2S_{1/2} \rightarrow 4S_{1/2}$ ,  $2S_{1/2} \rightarrow 4P_{1/2}$ , and crossover region were recorded in the usual way alternating between the hydrogen and deuterium lines. This was done at several discharge pressures to ensure that the two had the same systematic shifts. The spectra were analyzed in the standard manner.

## V. RESULTS

### A. Systematic shifts of the 1S-2S line

In this and all subsequent sections, numerical results are given in terms of the fundamental dye-laser frequency unless otherwise stated. All systematic line shifts are given as  $\nu$  (measured) -  $\nu$  (true).

The 1S-2S pressure shift was determined to be less than 5 MHz/torr, and since the isotope and Lamb-shift measurements were made at 0.5 torr this caused a negligible correction and uncertainty to the result.

The ac Stark effect<sup>20</sup> was estimated by measuring the 2430-Å beam size ( $0.02 \times 0.04$  cm<sup>2</sup>) and peak power (0.9-1.1 kw) and using the result in Ref. 21 of 0.6 Hz/W/cm shift. This gave a shift of  $0.8 \pm 0.2$  MHz.

The largest uncertainty in the results is caused by the difficulty to relate the line shape of the two-photon signal to the true atomic transition frequency. The atomic linewidth of the 1S-2S transi-

tion can certainly be neglected compared to the laser bandwidth. In linear spectroscopy the observed line shape would then simply be given by the laser intensity spectrum, which can be readily measured with a spectrum analyzer. For two-photon excitation, however, the calculation of the line shape,  $P(\omega')$ , involves the convolution of the field spectrum,

$$P(\omega') \propto \left| \int E(\omega) E(\omega' - \omega) d\omega \right|^2, \quad (6)$$

where  $E(\omega)$  is the component of the electric field of the laser at frequency  $\omega$ . A serious problem arises now, because this integral depends on the relative phases as well as the amplitudes of the field components, whereas an optical spectrum analyzer can determine only the intensity or amplitude. In the present experiment the situation is aggravated because there are two nonlinear processes, frequency doubling and two-photon excitation, which can each introduce uncertain line shifts and distortions between the measured laser intensity spectrum and the observed two-photon signal.

If the relative phases in the amplitude spectrum were truly arbitrary one could create almost any signal line shape. But fortunately the possible phase variations in the present experiment are quite limited by the origin of the laser pulse. We have used various models for these phase variations, together with the measured laser intensity spectrum, to numerically calculate possible two-photon line shapes. By comparing the calculated and observed line shapes we have determined which model gives the best agreement and have used this model to estimate a correction to the observed transition frequency. We have also considered which models correspond to realistic extremes for the possible phase variations, and have used the corresponding corrections to set our uncertainty.

The interferometer in Fig. 4 measures the pulsed laser intensity spectrum and relates it to the cw laser frequency. For an ideal laser amplifier this spectrum would be Gaussian, with a Fourier-transform-limited linewidth determined by the pulse length. In this case, there would be no phase variation and the peak frequency would be the same as that of the cw laser. The observed spectrum, however, appeared downshifted in its peak frequency by 17 MHz, the linewidth was almost twice as large as the transform limit, and the line shape appeared slightly asymmetric with a small but long tail on the low frequency side. This would imply a shift of the measured 1S-2S frequency of -68 MHz.

If the phases varied rapidly and randomly from one frequency interval to the next, the square of

the convolution integral<sup>6</sup> could be replaced by a convolution integral of the intensity spectrum. In this limit there would be no shift between the atomic frequency and the peak of the observed signal. The line profile calculated for this case, however, was 20% narrower and more symmetric than our observed line.

Next we investigated the (also quite unrealistic) limit of zero phase variations across the amplitude spectrum, given by the square root of the intensity spectrum. In this case the calculated line profile was drastically skewed, due to the long tail in the spectrum, and had little resemblance to the observed line.

Since the long tail is, in all likelihood, due to some brief, rapid frequency chirping, it seemed more realistic to remove this tail and to assume constant phase only for the remainder of the amplitude spectrum before computing the convolution integral. This approximation reproduced the observed line shape fairly well, although the calculated linewidth was about 10% too large. The predicted resonance peak had a lower frequency. As a case between these two limits we continued to assume a constant phase in the integrand of the convolution integral, but restricted the integration limits. The rationalization for this is that frequency components separated by much more than the Fourier-transform-limited width should be uncorrelated. The calculated peak shape and position is fairly insensitive to what is used as the central frequency of the integration. It matches the observed shape quite well when our limits are about 2.5 Fourier-transform-limited linewidths on either side of the frequency of maximum amplitude. In this case the predicted shift of the 1S-2S frequency is -40 MHz. Because our approach cannot be entirely rigorous we have cautiously chosen error bars which more than cover the discussed limiting cases, assuming a shift of  $-40 \pm 28$  MHz. The uncertainty of this shift is much larger than the  $\pm 3$ -MHz statistical limit. Of course, the corrections of the observed fundamental frequency are one quarter as large.

#### B. Systematic shifts of the Balmer- $\beta$ line

The largest correction to the position of the Balmer- $\beta$  reference line is that due to pressure and electric-field effects. The positions of the  $2S_{1/2} - 4P_{1/2}$  line and the  $4S_{1/2} - 2S_{1/2} - 4P_{1/2}$  crossover both changed linearly with the pressure to within the statistical accuracy ( $\sim 1$  MHz), although the shifts were due to both pressure and electric field. Taking advantage of that behavior we have extrapolated their positions to zero pressure. The shift from 0 to 0.27 torr is  $-17.0 \pm 3.4$  MHz for the  $2S_{1/2} - 4P_{1/2}$  peak and  $-7.6 \pm 1.6$  MHz for the

crossover, with the uncertainty primarily due to the inaccuracy of the pressure readings.

The residual "zero-pressure" electric field can be found by comparing the extrapolated separation between the two peaks with theoretical calculations. Knowing this field we can determine the residual Stark shift of the crossover line. Because the separation between the two peaks is approximately 4 times more sensitive to the electric field than the crossover position, the correction of the latter should have very little uncertainty.

One difficulty arises, though, because both the  $4S_{1/2}$  state and the  $4P_{1/2}$  state possess unresolved hyperfine structure, and we do not know with certainty to what extent the hyperfine interaction is decoupled by collisions in the discharge plasma. Weber and Goldsmith<sup>22</sup> have found in later investigations of the hydrogen Balmer- $\alpha$  line that the hyperfine splitting of the  $3P_{1/2}$  state is almost completely destroyed at helium pressures above 0.1 torr. Unresolved hyperfine splitting is of little consequence in linear spectroscopy where it does not shift the center of gravity of a spectral line. In polarization spectroscopy, however, we expect, in general, some line displacement due to unresolved hyperfine structure, and collisional decoupling can lead to measurable line shifts.

In order to consider two limits we have calculated the Stark shift  $n=4$  energy levels as a function of electric field by numerically diagonalizing the Hamiltonian<sup>23</sup> without and with inclusion of hyperfine interaction. A comparison of calculated polarization spectra with the extrapolated observed separation between the two peaks yields a zero-pressure electric field of  $4.3 \pm 0.1$  V/cm if hyperfine interactions can be ignored. The corresponding Stark shift of the crossover position

amounts to  $-2.6 \pm 0.2$  MHz. If the hyperfine splitting were fully present the calculated zero-pressure field would equal  $4.6 \pm 0.2$  V/cm and the combined Stark and hyperfine shift of the crossover would be  $-6.5 \pm 0.2$  MHz. The error bars in the final analysis are chosen large enough to span both limits.

Including the pressure shifts discussed earlier we then arrive at a total shift of  $-12.2 \pm 2.6$  MHz for the position of the crossover line. The ac Stark effect at a beam intensity of  $5 \pm 2$  W/cm<sup>2</sup> causes a calculated additional shift of  $-1.4 \pm 0.5$  MHz of the crossover position. No shift of the line with discharge current between 11 and 20 mA was observed within the statistical error limits.

### C. Hydrogen 1S Lamb shift

The hydrogen ground-state Lamb shift is found from the separation between the Balmer- $\beta$  crossover line ( $4S_{1/2 F=0,1} - 2S_{1/2 F=1} - 4P_{1/2 F=0,1}$ ) and the  $1S_{F=1} - 2S_{F=1}$  two-photon line, recorded at the fundamental dye-laser frequency. Under the experimental conditions described in Sec. IV D we measure a separation  $\Delta\nu = \nu$  ( $H_\beta$  crossover)  $- \nu(1S-2S)/4$  of  $4760.4 \pm 1.2$  MHz. After applying the systematic corrections summarized in Table II, we arrive at a true separation of  $4764.8 \pm 7.6$  MHz.

The theoretical separation, including all terms (7) except for the 1S Lamb shift, is 2727.0 MHz. From a comparison, we find a 1S Lamb shift of  $8151 \pm 30$  MHz, which is in excellent agreement with the theoretical value<sup>7</sup> of  $8149.43 \pm 0.08$  MHz. The experimental uncertainty is dominated by the frequency shift introduced by the pulsed dye-laser amplifiers.

TABLE II. Separation  $\Delta\nu = \nu$  ( $H_\beta$  crossover)  $- \nu(1S-2S)/4$ .

Raw measurement (statistical average from 45 two-photon spectra at 0.05 torr, 51 Balmer- $\beta$ spectra at 0.27 torr, 11 mA)	4760.4 $\pm$ 1.2 MHz
Systematic corrections	
(a) 1S-2S line	
laser line shape	-10.0 $\pm$ 7.0 MHz
ac Stark effect	+0.8 $\pm$ 0.1
(b) Balmer- $\beta$ line	
pressure, electric field, hyperfine structure	12.2 $\pm$ 2.6 MHz
ac Stark effect	1.4 $\pm$ 0.5
total correction	4.4 $\pm$ 7.5 MHz
corrected separation $\Delta\nu$	4764.8 $\pm$ 7.6 MHz

#### D. Hydrogen-deuterium 1S-2S shift

The 1S-2S isotope shift could be measured with much less systematic uncertainty because the two-photon line shape was the same for hydrogen and deuterium. We found an experimental separation of  $670992.3 \pm 6.3$  MHz between the two line centroids. This result is in good agreement with the theoretical prediction<sup>7</sup> of  $670994.96 \pm 0.81$  MHz and is about ten times more precise than that of the best previous experimental value.<sup>3</sup> This result is of interest in its own right because it gives the first confirmation of the predicted relativistic nuclear recoil corrections [Eq. (2)].

#### E. Balmer- $\beta$ isotope shift and deuterium 1S Lamb shift

The isotope shift between the  $2S_{1/2F=1} \rightarrow 4P_{1/2F=0,1}$  component of the Balmer- $\beta$  line was measured to be  $167783.9 \pm 1.2$  MHz. No systematic dependence on pressure or voltage could be detected, since both isotopes are affected in nearly the same way. A correction of  $+0.7 \pm 0.7$  MHz has been included, though, to allow for a difference in unresolved  $4P$  hyperfine splitting, as discussed in Sec. IV B. The result agrees with the theoretical value<sup>7</sup> of  $167783.7 \pm 0.2$  MHz.

The Balmer- $\beta$  isotope shift, together with the 1S-2S isotope shift and the hydrogen 1S Lamb shift has been used to derive an experimental deuterium 1S Lamb shift of  $8177 \pm 30$  MHz in agreement with the theoretical result<sup>7</sup> of  $8172.23 \pm 0.12$  MHz.

### VI. CONCLUSIONS AND FUTURE IMPROVEMENT

Using laser spectroscopic techniques we have measured the 1S Lamb shift in hydrogen and deuterium with improved precision and we find good agreement with theory. We have also improved the measurement of the 1S-2S hydrogen-deuterium isotope shift and find it too agrees with theory; it agrees, in particular, with the predicted relativistic nuclear recoil correction which has never

before been tested.

The techniques used offer the possibility of considerable improvements in both these measurements. In traditional excited-state Lamb-shift measurements, the broad  $P$  state linewidth has always limited the possible precision. Our approach does not have this limitation. With purely technical improvements, such as better lasers and hydrogen atomic beams it could far surpass the precision of present measurements of any Lamb shift.

It should, for instance, be possible to achieve a Balmer- $\beta$  reference linewidth as narrow as 1 MHz by observing the 2S-4S dipole-forbidden line component in a two-step process (one optical photon + one radiofrequency photon),<sup>24</sup> or simply by single-photon transitions in the presence of a weak electric field. The two-photon linewidth could be reduced by using a laser amplifier of longer pulse duration, or by using the technique of multiple pulse excitation.<sup>25,26</sup>

It would be particularly interesting to improve the 1S-2S isotope shift measurement because the present theoretical uncertainty is limited by the electron-to-proton-mass ratio, and thus an improved experiment could be used to obtain a better value for this ratio.

#### ACKNOWLEDGMENTS

We are indebted to Dr. John E. M. Goldsmith for a computation of the hydrogen Stark effect, taking into account hyperfine interactions. We are also grateful to Professor Arthur L. Schawlow for his stimulating interest in this work, and we thank Frans Alkemade and Kenneth Sherwin for skilled technical assistance. Finally we would like to thank Dr. Dirk J. Kuizenga for lending us a superb acousto-optic frequency shifter of his design. This work was supported by the National Science Foundation under Grant No. NSF 9687, and by the Office of Naval Research under Contract No. ONR N00014-78-C-0403.

\*Present address: Randall Laboratory of Physics, University of Michigan, Ann Arbor, Michigan 48105.

<sup>1</sup>W. E. Lamb, Jr. and R. C. Retherford, *Phys. Rev.* **79**, 549 (1950).

<sup>2</sup>T. W. Hänsch, S. A. Lee, R. Wallenstein, and C. Wieman, *Phys. Rev. Lett.* **34**, 307 (1975).

<sup>3</sup>S. A. Lee, R. Wallenstein, and T. W. Hänsch, *Phys. Rev. Lett.* **35**, 1262 (1975).

<sup>4</sup>C. Wieman and T. W. Hänsch, *Phys. Rev. Lett.* **36**, 1170 (1976).

<sup>5</sup>G. Herzberg, *Proc. R. Soc. London, Ser. A* **234**, 516 (1956).

<sup>6</sup>T. W. Hänsch, M. H. Nayfeh, S. A. Lee, S. M. Curry, and I. S. Shahin, *Phys. Rev. Lett.* **32**, 1336 (1974).

<sup>7</sup>G. W. Erickson, *J. Phys. Chem. Ref. Data* **6**, 831 (1977).

<sup>8</sup>T. W. Hänsch, in *Tunable Lasers and Applications*, edited by A. Mooradian *et al.*, Springer Series in Optical Sciences (Springer, New York, 1976), Vol. 3, p. 326.

<sup>9</sup>T. W. Hänsch, *Phys. Today* **30**, 34 (1977).

<sup>10</sup>N. Bloembergen and M. D. Levenson, in *High Resolution Laser Spectroscopy*, Topics in Applied Physics (Springer, New York, 1976), Vol. 13, p. 315.

<sup>11</sup>L. S. Vasilenko, V. P. Chebotayev, and A. V. Shishaev,

- Pis'ma Zh. Eksp. Teor. Fiz. 12, 161 (1970) [JETP Lett. 12, 113 (1970)].
- <sup>12</sup>Y. Gontier and M. Trahin, Phys. Lett. 36A, 463 (1971).
- <sup>13</sup>F. Bassani, J. J. Forney, and A. Quattropiani, Phys. Rev. Lett. 39, 1070 (1977).
- <sup>14</sup>T. W. Hänsch, in *Proceedings of the International School of Physics "Enrico Fermi," Course LXIV on Nonlinear Spectroscopy, Varenna, Italy, 1975* (North-Holland, New York, 1977), p. 17.
- <sup>15</sup>T. W. Hänsch, M. D. Levenson, and A. L. Schawlow, Phys. Rev. Lett. 26, 946 (1971).
- <sup>16</sup>F. V. Kowalski, R. T. Hawkins, and A. L. Schawlow, J. Opt. Soc. Am. 66, 965 (1976).
- <sup>17</sup>R. Wallenstein and T. W. Hänsch, Opt. Commun. 14, 353 (1975).
- <sup>18</sup>W. L. Fites, R. T. Brackman, D. G. Hummer, and R. F. Stebbings, Phys. Rev. 116, 363 (1959); 124, 2051 (1961).
- <sup>19</sup>T. W. Hänsch, I. S. Shahin, and A. L. Schawlow, Phys. Rev. Lett. 27, 707 (1971).
- <sup>20</sup>A. M. Bonch-Bruевич and V. A. Khodovoi, Usp. Fiz. Nauk 93, 71 (1967) [Sov. Phys. Usp. 10, 637 (1968)].
- <sup>21</sup>S. A. Lee, Ph.D. thesis, Stanford University, M. L. Report No. 2460 (1975).
- <sup>22</sup>E. W. Weber and J. E. M. Goldsmith, Phys. Lett. 70A, 95 (1979).
- <sup>23</sup>G. Urders, Ann. Phys. (Leipzig) 6, 308 (1951).
- <sup>24</sup>E. W. Weber and J. E. M. Goldsmith, Phys. Rev. Lett. 41, 940 (1978).
- <sup>25</sup>R. Teets, J. N. Eckstein, and T. W. Hänsch, Phys. Rev. Lett. 38, 760 (1977).
- <sup>26</sup>J. N. Eckstein, A. I. Ferguson, and T. W. Hänsch, Phys. Rev. Lett. 40, 847 (1978).